Atmos. Chem. Phys. Discuss., 5, 9065–9096, 2005
www.atmos-chem-phys.org/acpd/5/9065/
SRef-ID: 1680-7375/acpd/2005-5-9065
European Geosciences Union

Atmospheric Chemistry and Physics Discussions

Model simulations and aircraft measurements of vertical, seasonal and latitudinal O_3 and CO distributions over Europe

H. Fischer[1], M. Lawrence[1], Ch. Gurk[1], P. Hoor[1], J. Lelieveld[1], M. I. Hegglin[2], D. Brunner[2], and C. Schiller[3]

[1]Max Planck Institute for Chemistry, Airchemistry Division, P.O. Box 3060, 55020 Mainz, Germany
[2]Institute for Atmospheric and Climate Science, Swiss Federal Institute of Technology, Zurich, Switzerland
[3]FZ Jülich, ICG-1, Jülich, Germany

Received: 20 July 2005 – Accepted: 1 September 2005 – Published: 22 September 2005

Correspondence to: H. Fischer (hofi@mpch-mainz.mpg.de)

Abstract

During a series of 8 measurement campaigns within the SPURT project (2001–2003), vertical profiles of CO and O_3 have been obtained at subtropical, middle and high latitudes over western Europe, covering the troposphere and lowermost stratosphere up to ~14 km altitude during all seasons. The seasonal and latitudinal variation of the measured trace gas profiles are compared to simulations with the chemical transport model MATCH. In the troposphere reasonable agreement between observations and model predictions is achieved for CO and O_3, in particular at subtropical and mid-latitudes, while the model overestimates (underestimates) CO (O_3) in the lowermost stratosphere particularly at high latitudes, indicating too strong simulated bi-directional exchange across the tropopause. By the use of tagged tracers in the model, long-range transport of Asian air masses is identified as the dominant source of CO pollution over Europe in the free troposphere.

1. Introduction

The distribution of ozone (O_3) in the troposphere is affected by downward transport from the stratosphere (e.g. Levy et al., 1985; Holton and Lelieveld, 1996; Marcy et al., 2004) and local photochemistry (e.g. Crutzen, 1995; Lelieveld and Dentener, 2000). For a budget calculation of tropospheric O_3 at a given location, photochemical production and destruction, as well as transport in and out of the region have to be considered. This can only be achieved by 3-dimensional chemical transport models (CTM) or global circulation models (GCM), which need to be tested against observations from in-situ or remote sensing measurements (e.g. O'Connor et al., 2004; von Kuhlmann et al., 2003a). Although global observations of tropospheric O_3, carbon monoxide (CO) and nitrogen dioxide (NO_2), the latter being important O_3 precursors, have recently become available from satellite-based observations (Fishman et al., 1990; Borrell et al., 2003; Deeter et al., 2004; Buchwitz et al., 2004), the measurements are generally not verti-

cally resolved and refer to cloud-free conditions only, which limits their representativeness. Additionally, satellite retrievals must be validated against independent remote sensing or in-situ data. Furthermore, regular O_3 soundings are launched at various locations in the world (Logan, 1999), but they lack information about O_3 precursors.

In general, detailed information about profiles of O_3 and its precursors is thus only available from in-service and campaign-based aircraft measurements. The drawback of measurements from in-service aircraft, e.g. MOZAIC (Thouret et al., 1998), NOXAR (Brunner et al., 1998) and CARIBIC (Zahn et al., 2002) is, that trace gas profiles are often restricted to the vicinity of heavy-duty airports, and are thus not representative for the background atmosphere. On the other hand, campaign based data sets (for a recent compilation see: Emmons et al., 2000) usually provide limited information about seasonal and spatial variations. Here we present data from a series of airborne measurement campaigns made within the SPURT (SPURenstofftransport in der Tropopausenregion; Trace gas transport in the tropopause region) project (Engel et al., 2005). The major goal of SPURT was to obtain insight into the distribution of various trace gases in the free troposphere and lowermost stratosphere along the western border of Europe from the subtropics to the Artic during different seasons. We present results of 8 measurement campaigns, during which up to 6 flights were performed on two consecutive days in the period between November 2001 and July 2003. Here we focus on the data obtained during take-off and landing and compare average profiles of O_3 and CO for three latitude regimes and different seasons with simulations from the CTM MATCH-MPIC (Model of Atmospheric Transport and Chemistry – Max Planck Institute for Chemistry version). In the troposphere the distribution of both species is controlled by dynamical and photochemical processes so that they are particularly useful for the evaluation of chemistry transport models.

In Sect. 2 the SPURT measurements are described, while Sect. 3 presents a description of the MATCH model. In Sect. 4, the seasonal and latitudinal variations of in-situ profiles are compared to model results, while Sect. 5 addresses the origin of CO over Europe based on model simulations with tagged CO tracers. Finally, Sect. 6

summarizes the findings of our study.

2. Observations

A total of eight measurement campaigns covering all seasons were performed within SPURT between 10–11 November, 2001, 17–19 January, 2002, 16–17 May, 2002, 22–23 August, 2002, 17–18 October, 2002, 15–16 February, 2003, 27–28 April, 2003 and 9–10 July, 2003, respectively. All campaigns were flown out of the aircraft's home-base Hohn in northern Germany (54° N, 9° E). A typical campaign consisted of at least two southbound flights within one day, followed by two or more northbound flights performed on the next day. Thus a series of flights covered the latitude range between approximately 35° and 75° N along the western shore of Europe. During stop-over landings at generally smaller airports in the subtropics (Faro (Portugal, 37° N, 8° W); Casablanca (Morocco, 33° N, 7° W); Gran Canaria (28° N, 15° W); Lisbon (Portugal, 38° N, 9° W); Jerez (Spain, 36° N, 6° W); Monastir (Tunisia, 35° N, 10° E); Sevilla (Spain, 37° N, 5° W)) and at high northern latitudes (Kiruna (Sweden, 68° N, 20° E); Tromsö (Norway, 69° N, 18° E); Keflavik (Iceland, 64° N, 22° W); Longyearbyen (Norway, 78° N, 15° E)) two individual profiles between ground-level and approximately 14 km altitude were obtained during landing and take-off (Fig. 1).

Amongst others in-situ measurements of CO and O_3 were made on-board a Lear-Jet 35A (Engel et al., 2005; Hoor et al., 2004a). Carbon monoxide was measured by the MPI-C using Tunable Diode Laser Absorption Spectroscopy (TDLAS) (Kormann et al., 2002) with a time resolution of 1.3 s and a total uncertainty of less than 1.5%. Details of the CO measurements can be found in Hoor et al. (2004b). Ozone was measured independently by the FZ-Jülich using UV absorption (time resolution 9 s, total uncertainty 5%) and the ETH Zürich via NO chemiluminescence (time resolution: 1 s; total uncertainty: 5%) (Hegglin, 2004; Hegglin et al., 2005). A linear regression analysis showed that both measurements agree within their uncertainty bounds (O_3(CLD)=1.069 O_3(UV)+5.4 (ppbv), R^2=0.995; Hegglin, 2004). For the fol-

ACPD
5, 9065–9096, 2005

lowing analysis 5 s merged data sets have been calculated for each individual flight by averaging (CO, O_3(CLD)) and interpolation (O_3(UV)), respectively. From these merged data, mean profiles at subtropical (<40° N), mid- (approx. 52° N) and high latitudes (>65° N) have been calculated, grouped for the spring (March/April/May), summer (June/July/August), fall (September/October/November) and winter (December/January/February) seasons and 1 km altitude bins (0–1 km, 1–2 km, etc.).

3. Simulations

Average profiles for the different seasons and latitude bands were also deduced from model simulations, performed with the 3-D chemistry transport model MATCH-MPIC (Lawrence et al., 2003). The model is driven by meteorological data from the National Centre for Environmental Prediction (NCEP) Global Forecast System (GFS), and includes an extensive non-methane hydrocarbon oxidation mechanism described in detail by von Kuhlmann et al. (2003a). It is optimised for the troposphere and doesn't include stratospheric chemistry. Some compounds are adjusted or fixed in the stratosphere in order to provide boundary conditions to the troposphere. Values for H_2O, O_3, nitrogen compounds and methane are tied to observations from the HALO project (von Kuhlmann et al., 2003a). The model resolution is 2.8°×2.8° in the horizontal and includes 42 σ-levels in the vertical up to about 2 hPa. In addition to the extensive NMHC chemistry, the runs include regional CO tracers having the same emissions as the "standard" CO over a chosen region, subdivided into biomass burning and biofuel use, industrial and automotive sources, as well as other smaller sources like oceanic emissions, and undergo the same model transport and loss as standard CO. The emissions for CO and volatile organic compounds (VOC) from energy and industrial activities (except for biofuel use) were taken from the Emission Database for Global Atmospheric Research, EDGAR v2.0 for the VOCs (Olivier et al., 1996) and EDGAR v3.2 for CO and NO_x (Olivier et al., 2002). Biomass burning emissions (including biofuel use) were included by von Kuhlmann et al. (2003) based on the climatological CO emission distri-

bution of Galanter et al. (2000) and on the emission factors presented by Andreae and Merlet (2001). Here we use only the CO tracers for Asia (0° N–70° N, 60° E–180° E), N-America (15° N–75° N, 135° W–45° W) and Europe (35° N–75° N, 10° W–40° E), further separating between bio-fuel and automotive sources. The background CO is also calculated as two separate tracers from the photochemical oxidation of CH_4 and VOCs. Note that the sum of these two tracers is an accurate representation of the total chemical CO source, although the separation between CH_4 and VOCs is only approximate. To separate stratospheric O_3 from O_3 produced photochemically in the troposphere, an O_3(strat) tracer is used in the model, that marks ozone molecules of stratospheric origin, but undergoes the same chemistry and transport as total O_3. The model was run for the period June 2001 until February 2004. Individual profiles were obtained from the model at the locations and times of the individual SPURT profiles obtained during take-off and landing. From these, average profiles and 1σ-standard deviations (in 1 km altitude bins) were calculated.

4. Results

4.1. Seasonal and latitudinal variation of O_3 profiles

Average ozone profiles and 1σ-standard deviation for 1 km bins were calculated for low (<40° N), mid (~52° N) and high (>65° N) latitudes during the spring (March/April/May), summer (June/July/August), fall (September/October/November) and winter (December/January/February) seasons. These were obtained from at least 4 individual profiles per season and latitude band. In Fig. 2 observations are shown in red and MATCH model results in blue. Dashed blue curves indicate the modelled stratospheric contribution to O_3. In general, observations and simulations agree quite well within their combined 1σ-variability, with a few exceptions that will be discussed in detail below. Both observations and model results exhibit slightly increasing O_3 concentrations with altitude in the troposphere and a strong increase near the tropopause. Stratospheric

ACPD
5, 9065–9096, 2005

O_3 is highest in the winter and spring seasons at high northern latitudes (note the different scaling of the O_3-axis for low (0–400 ppbv), mid (0–600 ppbv) and high (0–1000 ppbv) latitudes in Fig. 2). This mirrors the seasonal and latitudinal variation of the tropopause height, which enables the aircraft to reach deeper into the stratosphere at high latitudes in winter and spring when the tropopause is lowest. Additionally, strong diabatic descent from the overworld fills the lowermost stratosphere with O_3-rich air during late winter/early spring (Hoor et al., 2004b, 2005; Hegglin et al., 2005). In general the model tends to overestimate stratospheric O_3 mixing ratios at low latitudes (Figs. 2a and g), underestimates it at high latitudes (Figs. 2c and f), while the agreement is best at mid-latitudes. This is most probably due to the coarse resolution of the model around the tropopause, which is about 30 hPa between 300 and 200 hPA, corresponding to an altitude resolution between 0.5 and 1 km. Thus slight differences in the tropopause height between actual observations and model predictions may lead to a vertical displacement between average modelled and observed profiles. In general, the model reproduces the observations quite well, with the exception of the summer profile at low latitudes (Fig. 2d), and the winter profiles in the mid- and upper troposphere (Figs. 2j–l). For summer conditions the model underestimates the O_3 concentration at low latitudes by approximately 30% (the mean observed and modelled O_3 between 3 and 9 km altitudes are 81±14 ppbv and 57±5 ppbv, respectively). Note that the MATCH model predicts that the stratospheric O_3 contribution between 3 and 9 km is only 30% of the modelled tropospheric O_3 concentration, the smallest value simulated for all profiles. This is no surprise, since the photochemical activity in the subtropics in summer is expected to be high, due to the generally cloud free conditions and high solar insolation over southern Europe (Lelieveld et al., 2002). Therefore, the discrepancy can be either due to an underestimation of transport of O_3 from the stratosphere, or an underestimation of the net O_3 production in the free troposphere by the model. A recent study by Jing et al. (2005) demonstrated that enhanced isentropic transport in summer across the subtropical jet leads to an ozone maximum in the upper troposphere of the subtropics, which is in agreement with our findings.

Too high O_3 in the troposphere is modelled for the winter profiles, in particular in the upper troposphere (Figs. 2j–l). Observed and modelled O_3 mixing ratios at 8.5 km are 51±14 ppbv, 48±5 ppbv, 71±26 ppbv and 99±31 ppbv, 116±28 ppbv, 118±27 ppbv for low, mid and high latitudes, respectively. Approximately 90% of the modelled O_3 at 8.5 km is predicted to originate from the stratosphere. Therefore it seems that MATCH either predicts a tropopause that is too low, or overestimates the transport of stratospheric air across the tropopause.

The seasonal and latitudinal variation of tropospheric O_3 is discussed in the following for the 5.5 km altitude bin, which is considered to be representative for the free troposphere, since it is neither influenced by small scale anomalies of the tropopause height nor by local emissions of O_3 precursors that generally take place in the boundary layer. Table 1 lists the mean and 1σ-standard deviation of observations and model results for the 5.5 km bin, at various seasons and latitudes. Additionally, the fractional contribution of stratospheric O_3 is listed. In general, seasonal and latitudinal variations of measured tropospheric O_3, at least in the middle troposphere, are remarkably small, varying between approximately 50 and 60 ppbv, with the exception of the summer profiles at low latitudes. If one takes into account that the solar irradiance - which drives photochemistry – strongly varies with season and latitude, the small variation of tropospheric O_3 is rather remarkable. While the highest O_3 mixing ratios at low latitudes are observed during the summer (80 ppbv), O_3 at mid and high latitudes peaks during the spring season (61–63 ppbv). The lowest mixing ratios are observed in winter at all latitudes (49–56 ppbv). The smallest variability is also observed in the winter seasons, consistent with observations by Logan (1999). The observed seasonal variation is at odds with the MATCH model simulations, predicting the highest concentrations in the winter (87–93 ppbv) due to strong O_3 import from the stratosphere. During the winter stratospheric O_3 contributes on average between 85 and 90% to tropospheric O_3 at 5.5 km. For the summer season MATCH underestimates the tropospheric O_3 concentration at low latitudes, when the stratospheric contribution is modelled to be minimum, ranging between 30% at low latitudes and 50% at high latitudes. As mentioned before,

this indicates that the exchange between the stratosphere and the troposphere is most probably too strong in MATCH, in particular for the winter, while net O_3 production at high solar irradiance is underestimated.

A comparison between observations and model results for the boundary layer is not possible since O_3 observations are often limited to altitudes above 2.5 km. Comparisons for the upper troposphere are difficult due to the averaging over different tropopause altitudes and are thus not discussed in detail here.

4.2. Seasonal and latitudinal variations of CO profiles

Figure 3 shows measured (black) and simulated (grey) CO profiles for the three latitude regimes during the four seasons. Additionally, CO tracers (coloured) are plotted to compare the contributions of photochemical CO production from CH_4 and VOCs (purple) with those of long range transport of primary CO emissions from Europe (green), North-America (red) and Asia (blue) (see Sect. 5).

In general, CO measurements and MATCH model simulations agree best in the middle and upper troposphere between approximately 3 and 10 km. At lower altitudes in the boundary layer, MATCH tends to underestimate CO mixing ratios. This is most probably due to local pollution at the airports, since boundary layer measurements are restricted to take-off and landing at various airports. In the middle and upper troposphere, simulations and observations agree within their combined 1σ-variability, with the exception of the summer profiles at mid and high latitudes (Figs. 3e and f) for which the observed CO mixing ratios are significantly higher than the model predictions. We will discuss these differences in more detail in the next section.

Above the tropopause in the lowermost stratosphere MATCH significantly overestimates the CO concentration. This is in line with the previously discussed underestimation of O_3 concentrations above the tropopause by MATCH attributed to excessive bi-directional stratosphere-troposphere-exchange (see Sect. 4.1). One possible explanation may be linked to the interpolation of NCEP vertical wind data to the MATCH coordinates, being sensitive to relatively small errors. Another potential reason is ex-

cessive numerical diffusion. Similar findings were described by Brunner et al. (2003) in an evaluation of five global CTM.

For a discussion of the seasonal and latitudinal variation of CO we again concentrate on the 5.5 km bin, which is not directly influenced by local pollution or direct stratospheric impact. Table 2 shows the average and 1σ-standard deviation of observed and simulated CO mixing ratios between 5 and 6 km altitude as a function of latitude and season. Middle tropospheric CO mixing ratios generally increase with latitude, reflecting the shorter photochemical lifetime associated with higher irradiance. This is in line with generally higher concentrations in winter/spring compared to summer. The latitudinal and seasonal variations deduced from the observations are reproduced by the model. Mean mixing ratios, and even the variability represented by the 1σ-standard deviations, are generally in excellent agreement, with the exception of the summer season at high latitudes, as mentioned before.

5. Photochemical CO production versus long range transport

In Fig. 3 the simulated CO profile is deconvoluted into various sources. The main contribution at all altitudes comes from photochemical CO production via oxidation of CH_4 and VOCs (purple line in Figs. 3a–l). This chemical background is of the order of 50 ppbv throughout the year and mainly due to the oxidation of CH_4. Contributions by long range transport of primary CO emissions (solid colour lines in Fig. 3 are total emissions from the combustion of fossil fuels and biomass burning, dashed lines represent biomass/biofuel burning only) from Europe, Asia, and North America individually are generally smaller than photochemical production. The largest contribution is attributed to Asian CO emissions (25 to 40 ppbv). This contribution is rather constant throughout the troposphere, with highest values in spring and lowest values in summer. Biofuel use and biomass burning constitute about 50% of the direct Asian CO emissions. Contributions by North American emissions are comparable to Asian sources in particular at altitudes below approximately 6 km, becoming less significant

ACPD
5, 9065–9096, 2005

at higher altitudes. The seasonal variation is less pronounced than for the Asian emissions and the contribution by biomass burning and biofuel use is generally small (less than 10 ppbv). European emissions are only significant at low altitudes, in particular at mid-latitudes, and decrease strongly with height.

A quantitative budget analysis is again obtained for the 5.5 km altitude bin (Fig. 4). The contribution from photochemistry (purple) is smallest in the winter and spring seasons (33–35%) at high latitudes and highest (56%) in summer at low latitudes. This is in line with the photochemical activity peaking at high solar irradiance in summer. Long-range transport of Asian emissions (blue) contributes 20–25% to the CO budget at 5.5 km at all latitudes and seasons, with the contributions of biofuel/biomass burning and fossil fuel combustion being approximately equal. North American emissions (red) account for 15–20% of the CO budget, with significant contributions from biomass burning only in the summer at high latitudes. European emissions (green) are highest during the summer at mid-latitudes (~15%), and smallest at low latitudes during all seasons (<10%).

This source apportionment is in quantitative agreement with a recent study by Pfister et al. (2004) using CO measurements from MOPITT and MOZART-2 CTM simulations to analyse the CO budget over Europe, indicating the robustness of our understanding of these budgets, i.e. within the limits of uncertainty in current global chemistry transport models.

As mentioned in the previous section MATCH underestimates the CO concentration in the middle troposphere during summer, particularly at middle and high latitudes. Most probably this is due to an underestimation of the biomass burning source from boreal forests fires in North America (Canada and Alaska). Kasischke et al. (2005) have shown that CO emissions from boreal fires in the summers of 2001 to 2003 (the SPURT period) were much higher than the climatological mean used in the MATCH simulations. Thus it is likely that MATCH underestimates CO in particular at mid and high latitudes in summer, most strongly affected by CO emissions from boreal fires (Yurganov et al., 2005).

6. Conclusions

Regular measurement flights have been performed in the upper troposphere and lower stratosphere along the western shores of Europe over a period of three years as part of the SPURT project. Stop-over landings at generally low-duty airports in low-, mid- and high-latitudes allow the study of seasonal and latitudinal variations of CO and O_3 profiles in the background atmosphere over Europe. The seasonal and latitudinal variations of the observations are in good agreement with earlier publications discussing O_3-sonde data (Logan, 1999) and satellite borne MOPITT CO data (Pfister et al., 2004). A comparison with simulations with the CTM MATCH indicates that the model tends to overestimate tropospheric O_3 in the winter season at all latitudes due to too strong stratosphere-troposphere exchange, and to underestimate photochemical O_3 production at high solar irradiance in the summer season at low latitudes. MATCH predicts that at least 50% of the tropospheric O_3 at 5.5 km originates in the stratosphere, with generally highest contributions in the winter season at high latitudes. The agreement between MATCH and observations for tropospheric CO is excellent, with the exception of high latitudes in the summer, when MATCH seems to underestimate the contribution of boreal forest fires to the CO budget. In agreement with the study by Pfister et al. (2004) the simulations indicate that approximately 50 ppbv of CO in the troposphere is due to photochemical production, mainly by the oxidation of CH_4, and to a lesser extent of VOCs, and that long-range transport of primary emissions from Asia is the most important CO pollution source over Europe.

Acknowledgements. We are indebted to the pilots and technicians at GFD, enviscope, MPIC, FZJ and ETH for their excellent cooperation and support during the campaigns. Funding of the SPURT project under the AFO 2000 programme of the German Ministry for Education and Research (BMBF) is gratefully acknowledged.

References

Andreae, M. O. and Merlet, P.: Emission of trace gases and aerosols from biomass burning, Global Biogeochem. Cycles, 15(4), 955–966, 2001.

Borrell, P., Burrows, J. P., Richter, A., Platt, U., and Wagner, T.: New developments in satellite capabilities for probing the chemistry of the troposphere, Atmos. Environ., 37, 2567–2570, 2003.

Brunner, D., Staehelin, J., and Jeker, D.: Large-scale nitrogen oxide plumes in the tropopause region and implications for ozone, Science, 282, 1305–1309, 1998.

Brunner, D., Staehelin, J., Rogers, H. I., Köhler, M. O., Pyle, J. A., Hauglustaine, D., Jourdain, L., Berntsen, T. K., Gauss, M., Isaksen, I. S. A., Meijer, E., van Velthoven, P., Pitari, G., Mancini, E., Grewe, V., and Sausen, R.: An evaluation of the performance of chemistry transport models by comparison with research aircraft observations. Part 1: Concepts and overall model performance, Atmos. Chem. Phys., 3, 1609–1631, 2003, SRef-ID: 1680-7324/acp/2003-3-1609.

Buchwitz, M., de Beek, R., Bramstedt, K., Noël, S., Bovensmann, H., and Burrows, J. P.: Global carbon monoxide retrieved from SCIAMACHY by WFM-DOAS, Atmos. Chem. Phys., 4, 1945–1960, 2004, SRef-ID: 1680-7324/acp/2004-4-1945.

Crutzen, P. J.: Ozone in the troposphere, in: Composition, Chemistry and Climate of Atmosphere, edited by: Singh, H. B., Van Nostrand Reinhold, New York, pp. 349–393, 1995.

Deeter, M. N., Emmons, L. K., Edwards, D. P., Gille, J. C., and Drummond, J. R.: Vertical resolution and information content of CO profiles retrieved by MOPETT, Geophys. Res. Lett., 31, L15112, doi:10.1029/2004GL020235, 2004.

Emmons, L. K., Hauglustaine, D. A., Müller, J.-F., Carroll, M. A., Brasseur, G. P., Brunner, D., Staehelin, J., Thouret, V., and Marenco, A.: Data composites of airborne observations of tropospheric ozone and its precursors, J. Geophys. Res., 105, 20 497–20 538, 2000.

Engel, A., Bönisch, H., Brunner, D., Fischer, H., Gurk, C., Hegglin, M., Hoor, P., Königstedt, R., Krebsbach, M., Maser, R., Parchatka, U., Peter, Th., Schiller, C., Schmidt, U., Spelten, N., Szabo, T., Weers, U., Wernli, H., Wetter, Th., and Wirth, V.: Highly resolved observations of trace gases in the lowermost stratosphere and upper troposphere from the SPURT project: An overview, Atmos. Chem. Phys. Discuss., 5, 5081–5126, 2005, SRef-ID: 1680-7375/acpd/2005-5-5081.

Fishman, J., Watson, C. E., Larsen, J. C., and Logan, J. A.: Distribution of tropospheric ozone determined from satellite data, J. Geophys. Res., 95, 3599–3617, 1990.

Galanter, M., Levy, H., and Carmichael, G. R.: Impacts of biomass burning on tropopsheric CO, NO_x and O_3, J. Geophys. Res., 105, 6633–6653, 2000.

Hegglin, M. I.: Airborne NOy-, NO and O_3-measurements during SPURT: Implications for atmospheric transport, Thesis No. 15553, Swiss Federal Institute for Technology (ETH), Zurich, Switzerland, 2004.

Hegglin, M. I., Brunner, D., Wernli, H., Schwierz, C., Martius, O., Hoor, P., Fischer, H., Parchatka, U., Spelten, N., Schiller, C., Krebsbach, M., Parchatka, U., Weers, U., Staehelin, J., and Peter, Th.: Tracing troposphere-to-stratosphere transport above a mid-latitude deep convective system, Atmos. Chem. Phys., 4, 741–756, 2004, SRef-ID: 1680-7324/acp/2004-4-741.

Hegglin, M. I., Brunner, D., Peter, Th., Hoor, P., Fischer, H., Staehelin, J., Krebsbach, M., Schiller, C., Parchatka, U., and Weers, U.: Measurements of NO, NO_y, N_2O, and O_3 during SPURT: implications for transport and chemistry in the lowermost stratosphere, Atmos. Chem. Phys. Discuss., 5, 8649–8688, 2005, SRef-ID: 1680-7375/acpd/2005-5-8649.

Holton, J. R. and Lelieveld, J.: Stratosphere-troposphere exchange and its role in the budget of tropospheric ozone, edited by: Crutzen, P. J. and Ramanathan, V., in: Clouds, Chemistry and Climate, NATO ASI Series, Springer-Verlag, Berlin, pp. 173–190, 1996.

Hoor, P., Bönisch, H., Brunner, D., Engel, A., Fischer, H., Gurk, C., Günther, G., Hegglin, M., Krebsbach, M., Maser, R., Peter, Th., Schiller, C., Schmidt, U., Spelten, N., Wernli, H., and Wirth, V.: New insights into upward transport across the extratropical tropopause derived from extensive in situ measurements during the SPURT project, SPARC Newsletter, 22, 29–31, 2004.

Hoor, P., Gurk, C., Brunner, D., Hegglin, M. I., Wernli, H., and Fischer, H.: Seasonality and extend of extratropical TST derived from in-situ CO measurements during SPURT, Atmos. Chem. Phys., 4, 1427–1442, 2004b, SRef-ID: 1680-7324/acp/2004-4-1427.

Hoor, P., Fischer, H., and Lelieveld, J.: Tropical and extratropical tropospheric air in the lowermost stratosphere over Europe: A CO-based budget, Geophys. Res. Lett., 32, L07802, doi:10.1029/2004GL022018, 2005.

Jing, P., Cunnold, D. M., Yang, E.-S., and Wang, H.-J.: Influence of isentropic transport on seasonal ozone variations in the lower stratosphere and subtropical upper troposphere, J. Geophys. Res., 110, D10110, doi:10.1029/2004JD005416, 2005.

Kasischke, E. S., Hyer, E. J., Novelli, P. C., Bruhwiler, L. P., French, N. H. F., Sukhinin, A. I., Hewson, J. H., and Stocks, B. J.: Influences of boreal fire emissions on Northern Hemisphere atmospheric carbon and carbon monoxide, Global Biogeochem. Cycles, 19, GB1012, doi:10.1029/2004GB002300, 2005.

Kormann, R., Fischer, H., Gurk, C., Helleis, F., Klüpfel, Th., Königstedt, R., Parchatka, U., and Wagner, V.: Application of TRISTAR, a three-laser tunable diode laser absorption spectrometer during MINATROC, Spectrochimica Acta, A58, 2489–2498, 2002.

Lawrence, M. G., Rasch, P. J., von Kuhlmann, R., Williams, J., Fischer, H., de Reus, M., Lelieveld, J., Crutzen, P. J., Schultz, M., Stier, P., Huntrieser, H., Heland, J., Stohl, A., Forster, C., Elbern, H., Jakobs, H., and Dickerson, R. R.: Global chemical weather forecasts for field campaign planning: Predictions and observations of large-scale features during MINOS, CONTRACE, and INDOEX, Atmos. Chem. Phys., 3, 267–289, 2003, SRef-ID: 1680-7324/acp/2003-3-267.

Lelieveld, J. and Dentener, F. J.: What controls tropospheric ozone?, J. Geophys. Res., 105, 3531–3551, 2000.

Lelieveld, J., Berresheim, H., Borrmann, S., Crutzen, P. J., Dentener, F. J., Fischer, H., de Gouw, J., Feichter, J., Flatau, P., Heland, J., Holzinger, R., Kormann, R., Lawrence, M., Levin, Z., Markowicz, K., Mihalopoulos, N., Minikin, A., Ramanathan, V., de Reus, M., Roelofs, G. J., Scheeren, H. A., Sciare, J., Schlager, H., Schultz, M., Siegmund, P., Steil, B., Stephanou, E., Stier, P., Traub, M., Williams, J., and Ziereis, H.: Global air pollution crossroads over the Mediterranean, Science, 298, 794–799, 2002.

Levy II, H., Mahlman, J. D., and Moxim, W. J.: Tropospheric ozone: The role of transport, J. Geophys. Res., 90, 3753–3772, 1985.

Logan, J. A.: An analysis of ozonesonde data for the troposphere: Recommendations for testing 3d-models and development of a gridded climatology for tropospheric ozone, J. Geophys. Res., 104(D13), 16 115–16 150, doi:10.1029/1998JD100096, 1999.

Marcy, T. P., Fahey, D. W., Gao, R. S., Popp, P. J., Richard, E. C., Thompson, T. L., Rosenlof, K. H., Ray, E. A., Salawitch, R. J., Atherton, C. S., Bergmann, D. J., Ridley, B. A., Weinheimer, A. J., Loewenstein, M., Weinstock, E. M., and Mahoney, M. J.: Quantifying stratospheric ozne in the upper troposphere with in situ measurements of HCl, Science, 304, 261–265,

2004.
O'Conner, F. M., Law, K. S., Pyle, J. A., Barjat, H., Brough, N., Dewey, K., Green, T., Kent, J., and Phillips, G.: Tropospheric ozone budget: Regional and global calculations, Atmos. Chem. Phys. Discuss., 4, 991–1036, 2004, SRef-ID: 1680-7375/acpd/2004-4-991.
Olivier, J. G. J., Bouwman, A. F., van de Maas, C. W. M., Berdowski, J. J. M., Veldt, C., Bloos, J. P. J., Visschedijk, A. J. H., Znadveld, P. Y. J., and Heverlag, J. L.: Description of EDGAR version 2.0: A set of emission inventories of greenhouse gases and ozone depleting substances for all anthropogenic and most natural sources on per country basis and on 1°×1° grid, Nat. Inst. Of Public Health and the Environ., Bilthoven, The Netherlands, 1996.
Olivier, J. G. J., Peters, J. A. H. W., Bakker, J., Berdowski, J. J. M., Visschedijk, A. J. H., and Bloos, J. P. J.: Applications of EDGAR: Emission data base for atmospheric research, Rep. 410.200.051.RIVM, RIVM, Bilthoven, The Netherlands, 2002.
Pfister, G., Petron, G., Emmons, L. K., Gille, J. C., Edwards, D. P., Lamarque, J.-F., Attie, J.-L., Granier, C., and Novelli, P.C.: Evaluation of CO simulations and the analysis of the CO budget for Europe, J. Geophys. Res., 109, D19304, doi:10.1029/2004JD004691, 2004.
Thouret, V., Marenco, A., Nedelec, P., and Grouhel, C.: Ozone climatologies at 9–12 km altitude as seen by the MOZAIC airborne program between September 1994 and August 1996, J. Geophys. Res. 103, 25 653–25 679, 1998.
von Kuhlmann, R., Lawrence, M. G., Crutzen, P. J., and Rasch, P. J.: A model for studies of tropospheric ozone and nonmethane hydrocarbons: Model description and ozone results, J. Geophys. Res., 108(D9), 4294, doi:10.1029/2002JD002893, 2003a.
von Kuhlmann, R., Lawrence, M. G., Crutzen, P. J., and Rasch, P. J.: A model for studies of tropospheric ozone and non-methane hydrocarbons: Model evaluation of ozone related species, J. Geophys. Res., 108(D28), 4729, doi:10.1019/2002JD003348, 2003b.
Yurganov, L. N., Duchatelet, P., Dzhola, A. V., Edwards, D. P., Hase, F., Kramer, I., Mahieu, E., Mellqvist, J., Notholt, J., Novelli, P. C., Röckmann, A., Scheel, H. E., Schneider, M., Schulz, A., Strandberg, A., Sussmann, R., Tanimoto, H., Velazco, V., Drummond, J. R., and Gille, J. C.: Increased Northern Hemispheric carbon monoxide burden in the troposphere in 2002 and 2003 detected from the ground and from space, Atmos. Chem. Phys., 5, 563–573, 2005, SRef-ID: 1680-7324/acp/2005-5-563.
Zahn, A., Brenninkmeijer, C. A. M., Asman, W. A. H., Crutzen, P. J., Heinrich, G., Fischer, H., Cuijpers, J. W. M., and van Velthoven, P. F. J.: Budgets of O_3 and CO in the upper

troposphere: CARIBIC passenger aircraft results 1997–2001, J. Geophys. Res., 107(D17), 4337, doi:10.1029/2001JD001529, 2002.

Table 1. Tropospheric ozone mixing ratios at 5.5 km altitude (Obs = observations; MATCH = model results; %-Str = stratospheric contribution).

Ozone 5.5 km	Low latitudes			Mid latitudes			High latitudes		
	Obs	MATCH	%-Str	Obs	MATCH	%-Str	Obs	MATCH	%-Str
Spring	58±6	65±6	56	61±20	66±11	63	63±10	81±8	76
Summer	80±11	56±2	30	54±13	64±7	42	67±13	61±2	50
Fall	52±3	67±4	77	53±8	56±4	69	57±3	56±8	64
Winter	49±6	87±24	85	50±3	93±12	90	56±2	92±10	92

Table 2. Tropospheric CO mixing ratios at 5.5 km altitude (Obs = observations; MATCH = model results).

CO 5.5 km	Low latitudes		Mid latitudes		High latitudes	
	Obs	MATCH	Obs	MATCH	Obs	MATCH
Spring	125±16	121±14	127±10	127±12	141±21	137±6
Summer	89±91	83±6	106±22	102±4	115±13	93±3
Fall	12±10	103±5	104±17	115±11	129±5	115±2
Winter	116±9	121±4	131±16	130±5	141±9	137±6

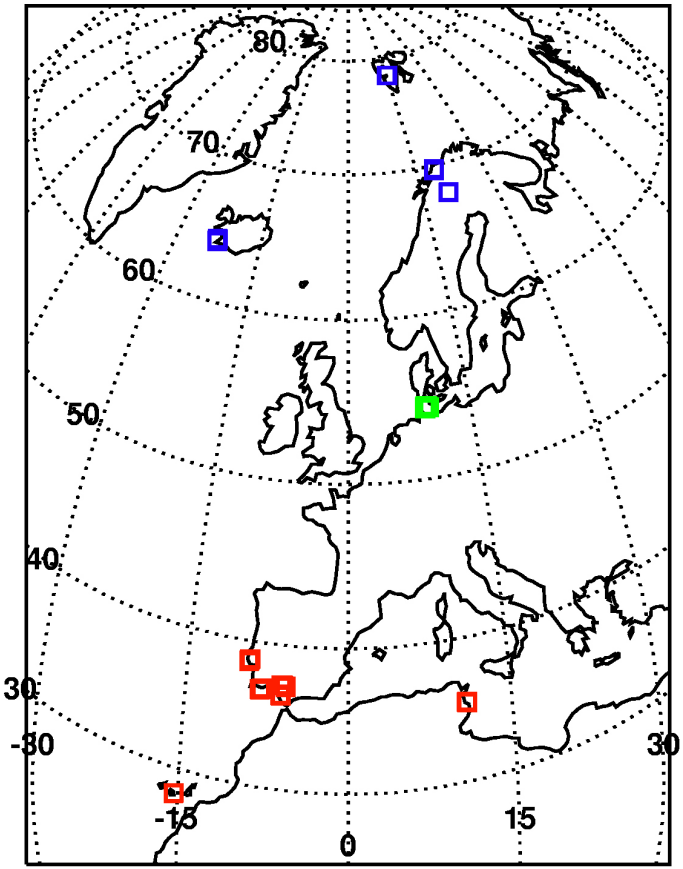

Fig. 1. Locations of the SPURT stop-over landings when profiles were flown. Low-latitude locations in red, mid-latitude in green and high latitude in blue.

ACPD

5, 9065–9096, 2005

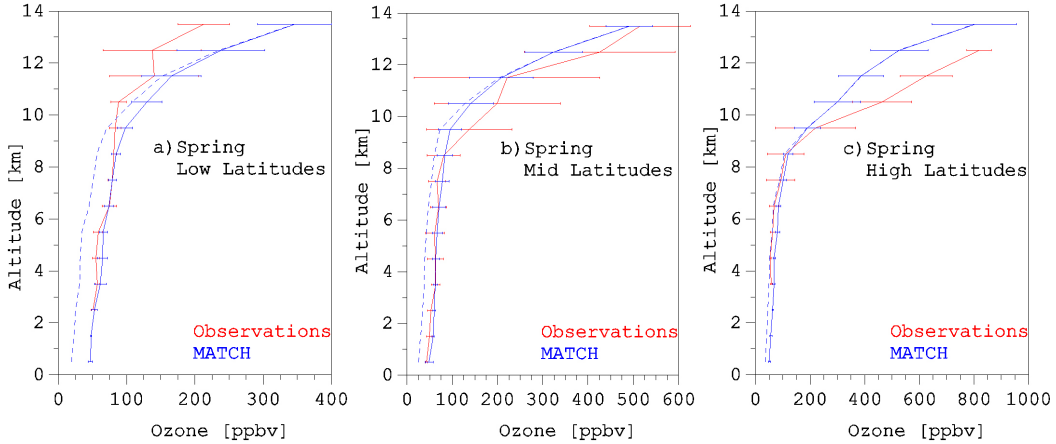

Fig. 2. Altitude profiles (mean and 1σ-standard deviation for 1 km altitude bins) of observed (red) and modelled (blue) O_3. The model estimate of tropospheric O_3 originating in the stratosphere is shown by the blue dotted line.

ACPD
5, 9065–9096, 2005

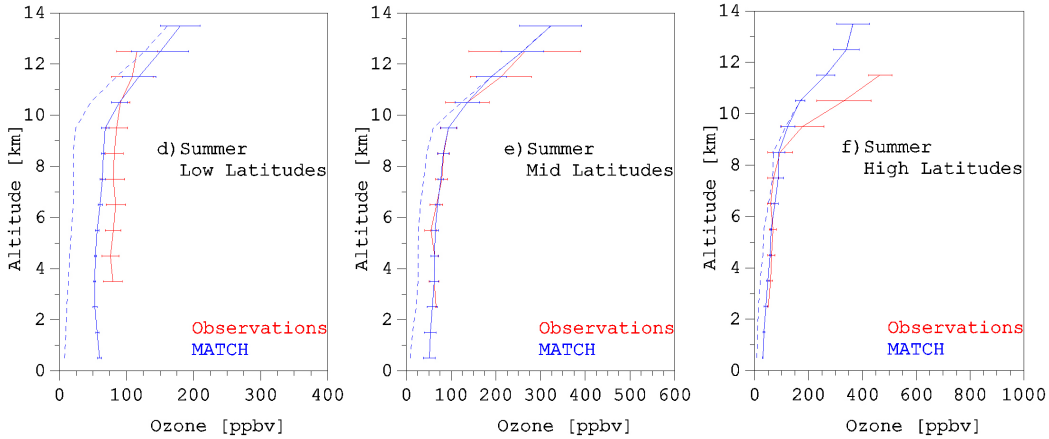

Fig. 2. Continued.

ACPD
5, 9065–9096, 2005

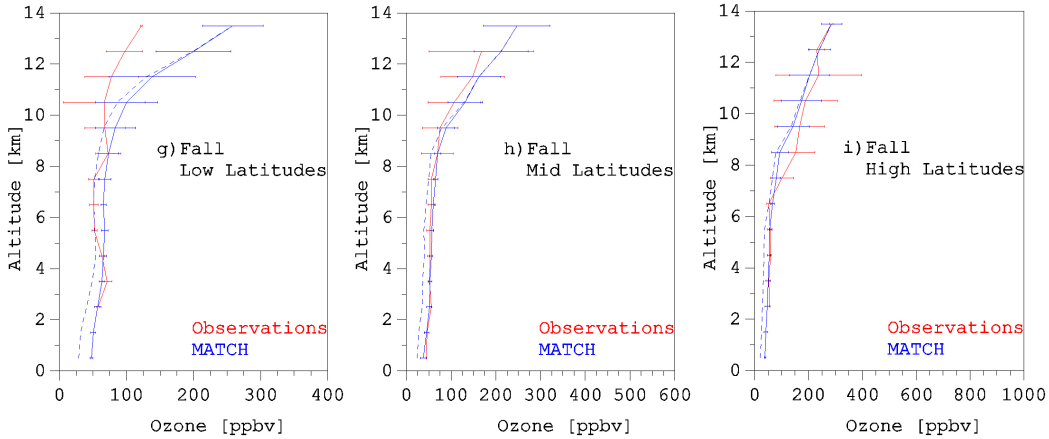

Fig. 2. Continued.

ACPD
5, 9065–9096, 2005

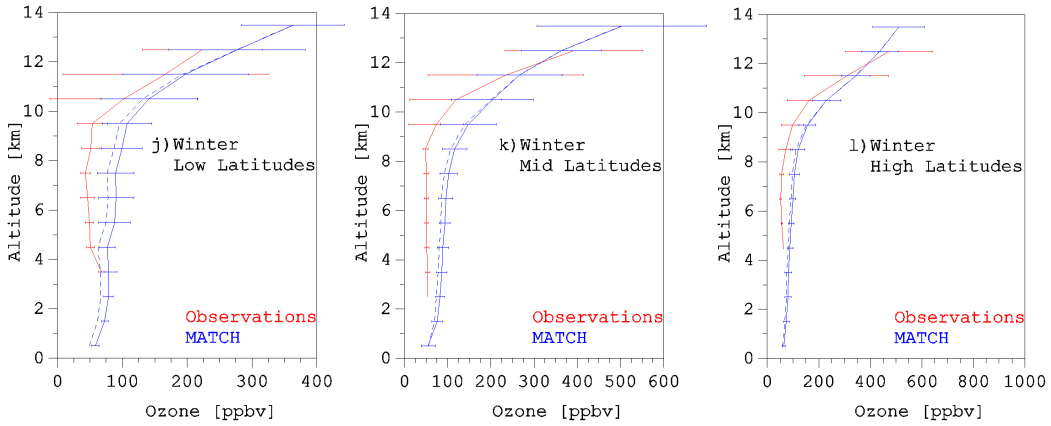

Fig. 2. Continued.

ACPD
5, 9065–9096, 2005

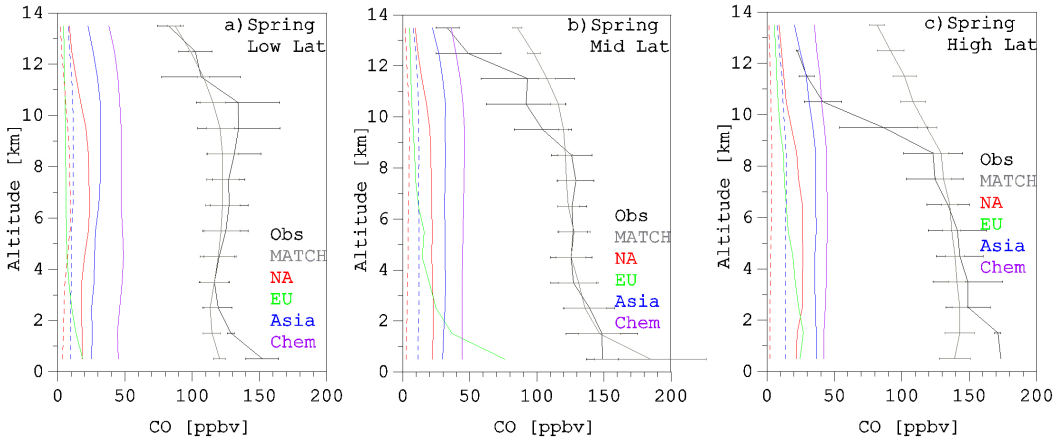

Fig. 3. Altitude profiles (mean and 1σ-standard deviation for 1 km altitude bins) of observed (black) and modelled (grey) CO. CO tracers are plotted to compare the contributions of photochemical CO production from CH_4 and VOCs (purple) with those by long-range transport of primary CO emissions (fossil fuel combustion and biomass burning) from Europe (green), North-America (red) and Asia (blue). Biomass burning contributions are plotted separately as coloured dashed lines.

ACPD
5, 9065–9096, 2005

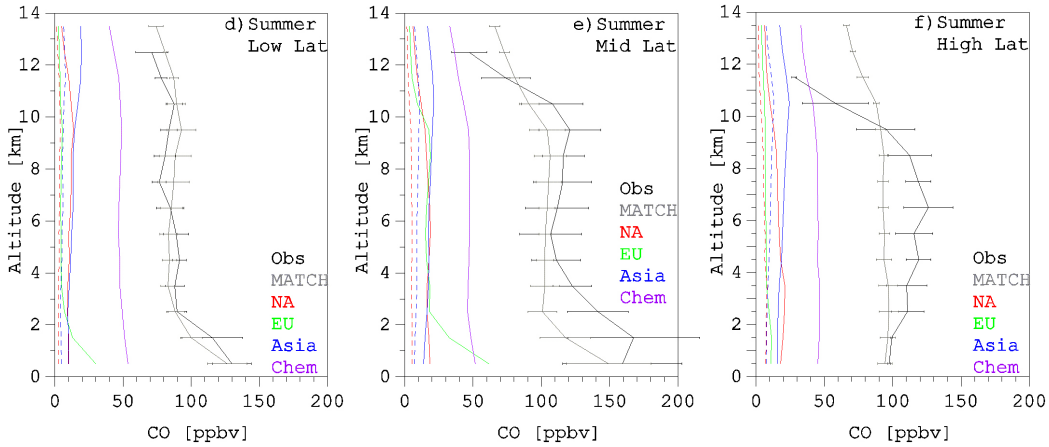

Fig. 3. Continued.

ACPD
5, 9065–9096, 2005

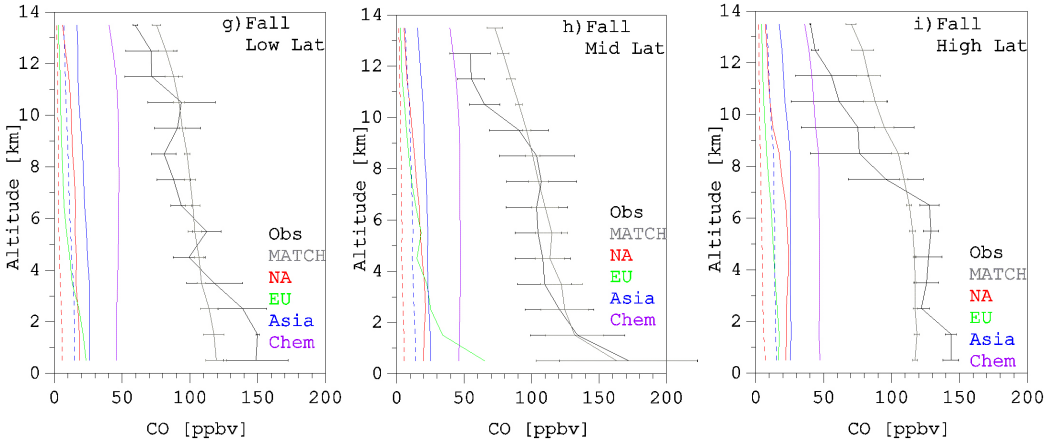

Fig. 3. Continued.

ACPD
5, 9065–9096, 2005

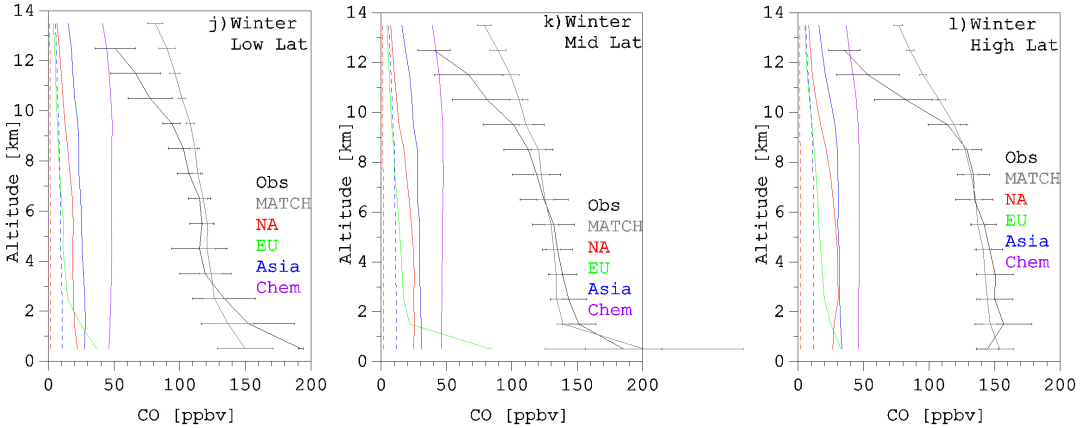

Fig. 3. Continued.

ACPD
5, 9065–9096, 2005

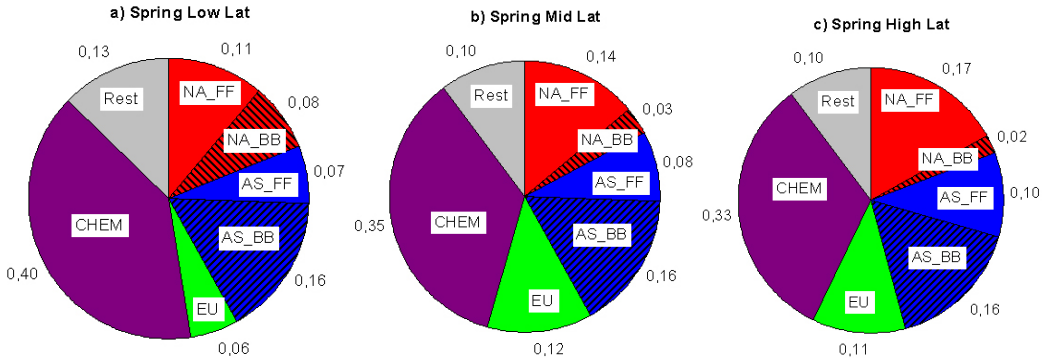

Fig. 4. CO budget calculated with MATCH at 5.5 km. Photochemical CO production is shown in purple, long-range transport of primary CO emissions form Europe, Asia and North-America are shown in green, blue and red, respectively. Darker (hatched) areas mark contributions from biomass burning and biofuel use. "Rest" summarises all other CO sources in the model.

ACPD
5, 9065–9096, 2005

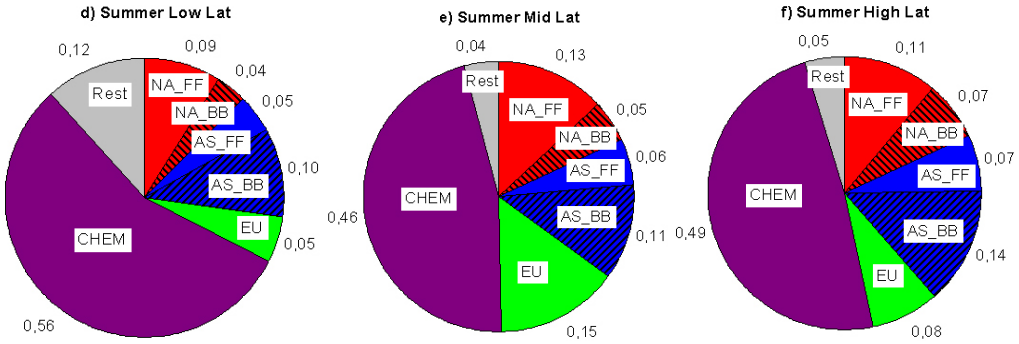

Fig. 4. Continued.

ACPD
5, 9065–9096, 2005

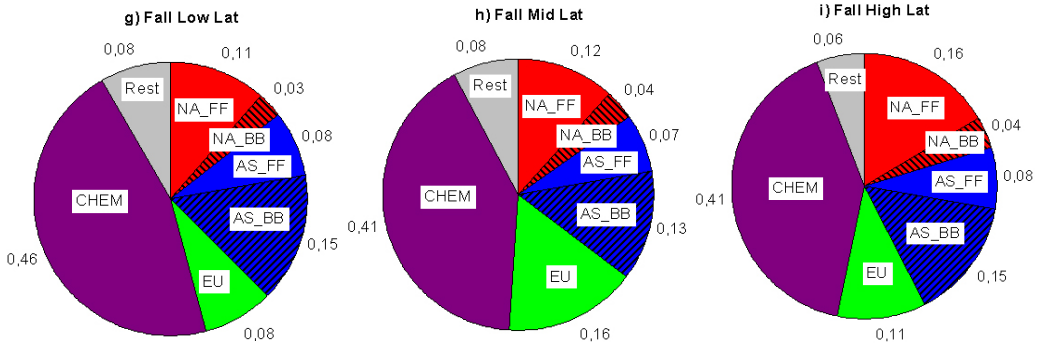

Fig. 4. Continued.

ACPD
5, 9065–9096, 2005

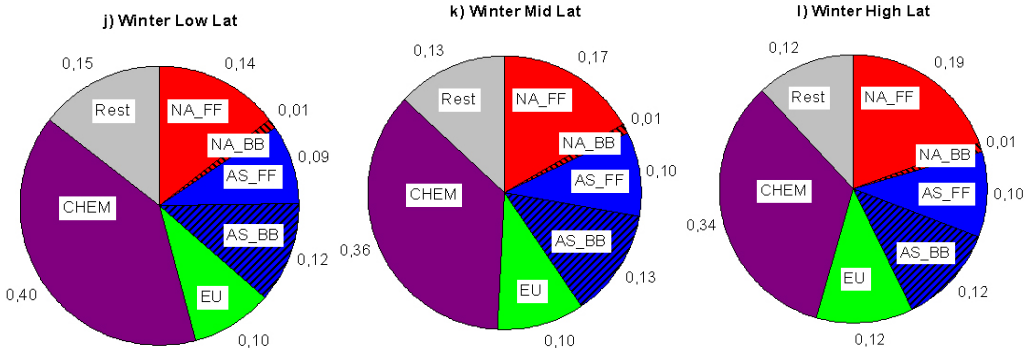

Fig. 4. Continued.

ACPD
5, 9065–9096, 2005